Journal of Geophysical Research Atmospheres

Supporting Information for

The Influence of Chemical and Mineral Compositions on the Parameterization of Immersion Freezing by Volcanic Ash Particles

N. S. Umo[1*], R. Ullrich[1], E. C. Maters[2†], I. Steinke[1‡], N. Benker[3], K. Höhler[1], R. Wagner[1], P. G. Weidler[4], G. A. Hoshyaripour[5], A. Kiselev[1], U. Kueppers[6], K. Kandler[3], D. B. Dingwell[6], T. Leisner[1], and O. Möhler[1]

1. Institute of Meteorology and Climate Research - Atmospheric Aerosol Research, Karlsruhe Institute of Technology, 76344 Eggenstein-Leopoldshafen, Germany.

2. Institute for Climate and Atmospheric Science, School of Earth and Environment, University of Leeds, Leeds LS2 9JT, United Kingdom.

3. Institute of Applied Geosciences, Technical University Darmstadt, 64287 Darmstadt, Germany.

4. Institute of Functional Interfaces, Karlsruhe Institute of Technology, 76344 Eggenstein-Leopoldshafen, Germany.

5. Institute of Meteorology and Climate Research, Department of Tropospheric Research, Karlsruhe Institute of Technology, 76344 Eggenstein-Leopoldshafen, Germany.

6. Department of Earth and Environmental Sciences, Ludwig-Maximilians-Universität, 80333 Munich, Germany.

*Correspondence to: Nsikanabasi Umo (nsikanabasi.umo@kit.edu)

† Department of Chemistry, University of Cambridge, Cambridge CB2 1EW, United Kingdom.

‡Atmospheric Sciences and Global Change Division, Pacific Northwest National Laboratory, Richland, WA99352, USA.

Contents of this file

Additional Supporting Information (Files uploaded separately)

Text S1. This supporting information includes figures and tables to support the discussion in the main article. A detailed description is given in the caption of each figure or table shown in this supporting information.

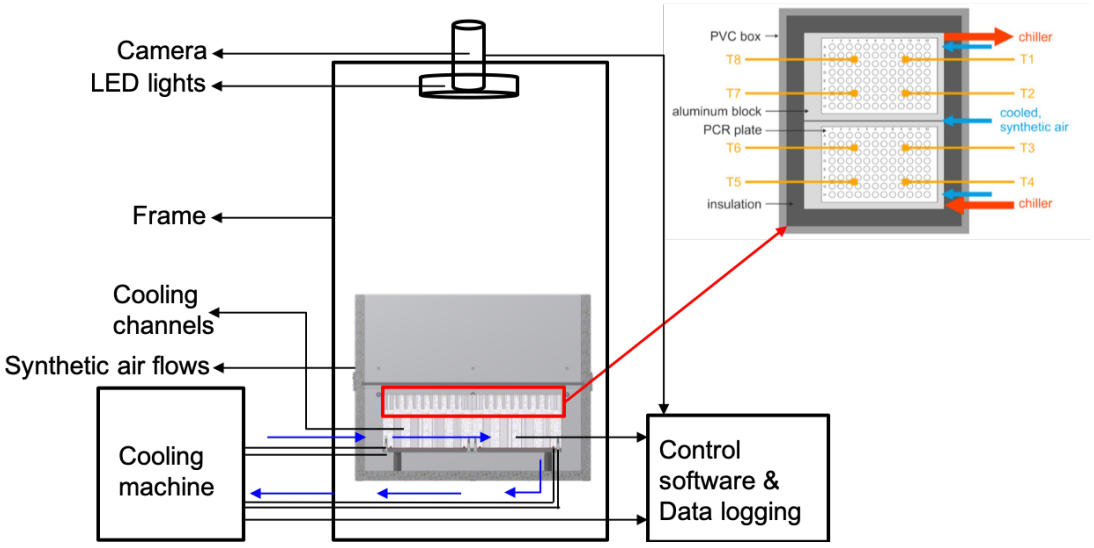

Figure S1. A schematic showing the INSEKT set-up. A more detailed description of this instrument and its operation is provided in the main manuscript.

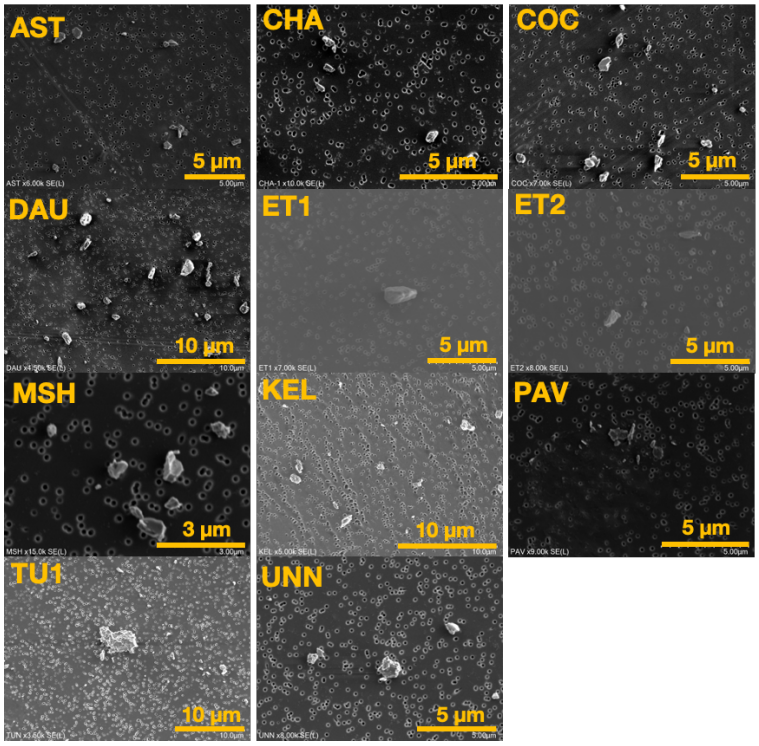

Figure S2. Images of volcanic ash (VA) particles from an analytical scanning electron microscope (ASEM, SU 5000 Schottky FE-SEM, HITACHI).

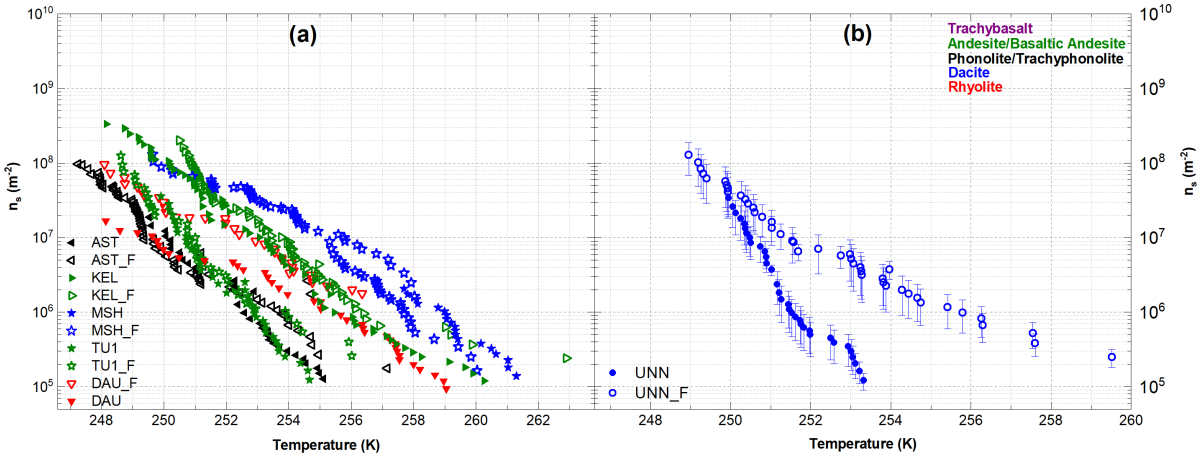

Figure S3. Comparison of n_s values of bulk and filter VA samples obtained from the INSEKT instrument. Error bars are not indicated in panel (a) for the sake of clarity. The uncertainties are similar to those shown in panel (b).

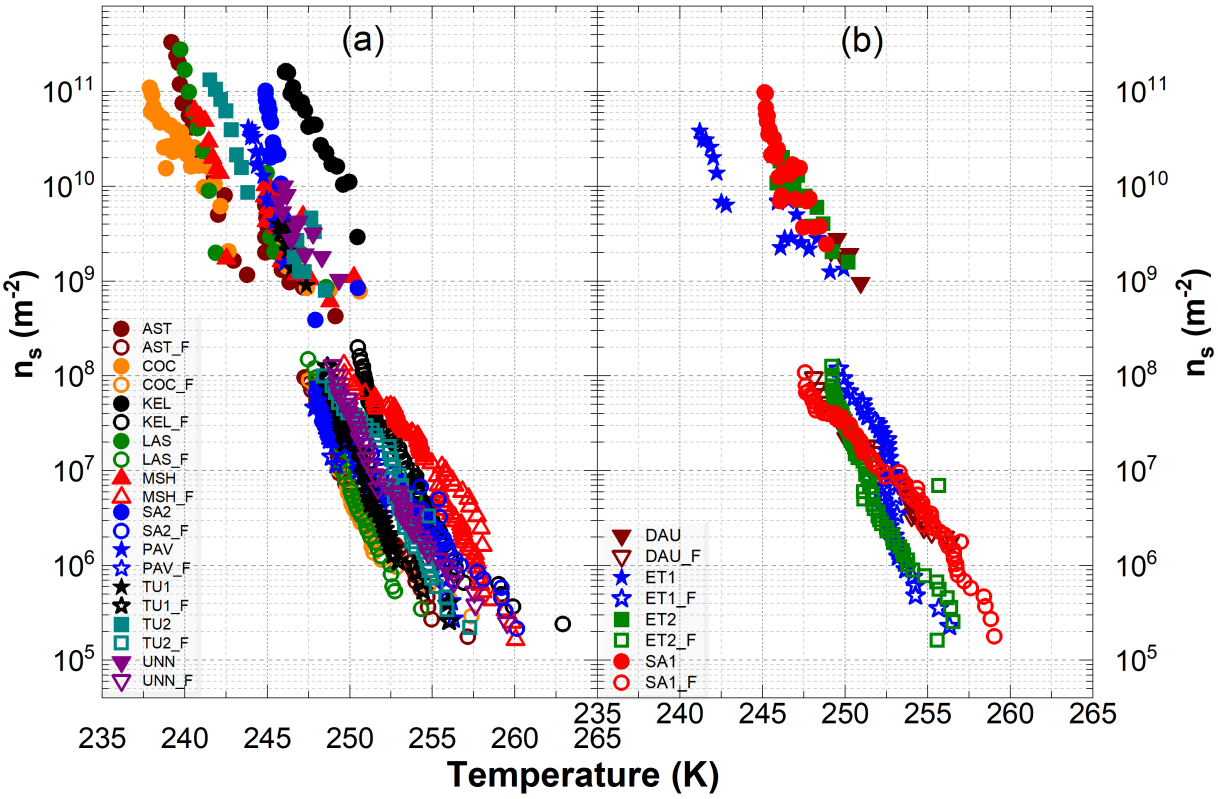

Figure S4. Comparison of n_s values of INSEKT analysis of filter samples (open symbols, wet suspension method) and AIDA (solid symbols, dry dispersion method) experiments. Error bars are not indicated in both panels for the sake of clarity. The uncertainties are similar to the error bars shown in Figure 9 (main manuscript) and Figure S3. The CHA sample is not included here because there was no INSEKT filter data to compare with.

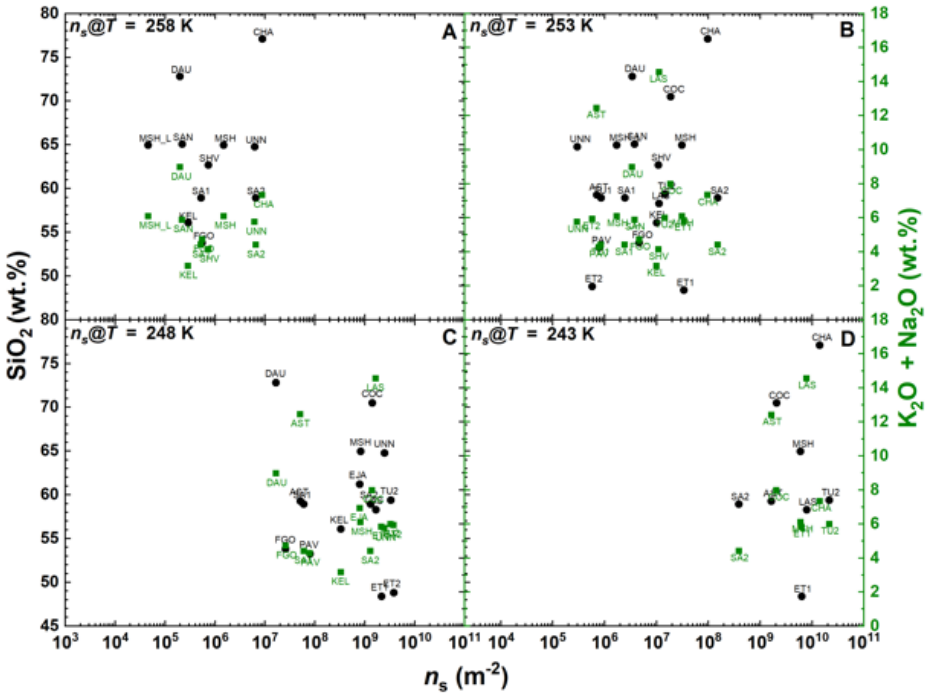

Figure S5. Pearson's correlation of n_s values at specific temperatures with chemical compositions of the VA particles. n_s values at T = 258 K, 253 K, 248 K, and 243 K are represented here. Correlation of n_s values with silicon dioxide (SiO_2, wt %, black circles) and with total alkali oxides (K_2O + Na_2O, wt%, green squares).

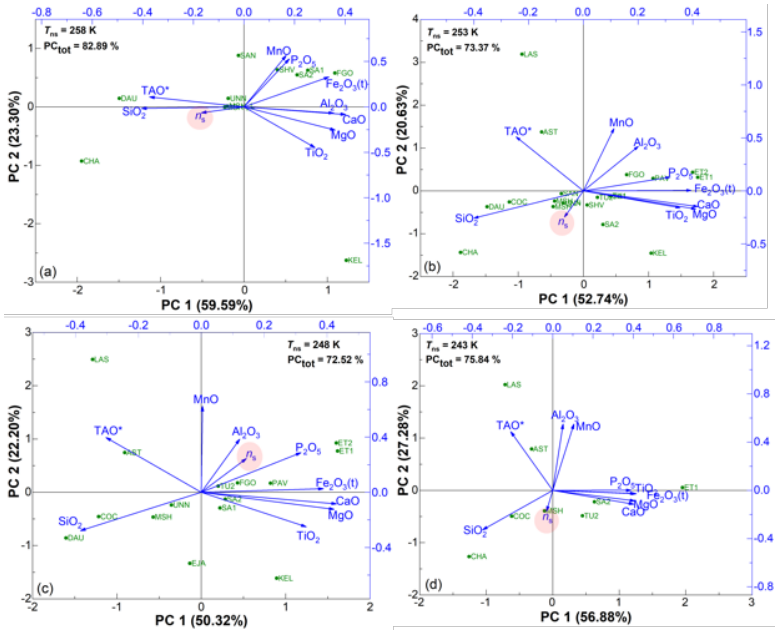

Figure S6. Principal component analyses of chemical oxide compositions of VA samples and their ice-nucleating abilities at different temperatures – T_{ns} = 258 K, 253 K, 248 K, and 243 K. The green dots show different VA samples that were analysed. The PC_{tot} indicates the percentage of components that were explained by the principal components (PC1 and PC2).

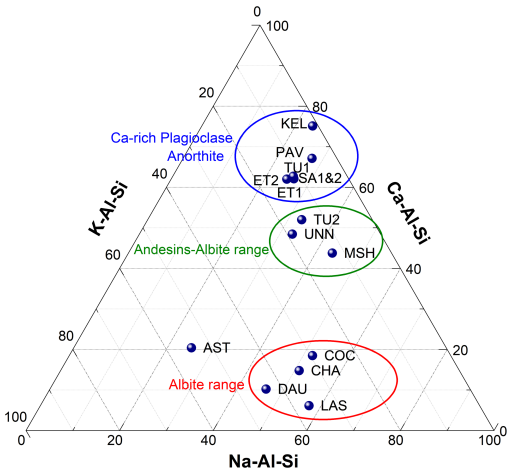

Figure S7. Detailed classification of the feldspar composition of the VA particles. The groupings are based on Na-Al-Si, K-Al-Si, and Ca-Al-Si compositions of the VA samples. The 15 VA samples are grouped into Ca-rich plagioclase anorthite (blue circle), andesine-albite (green circle), and the albite range (red circle).

Samples	Sample codes	Chemical oxides (%)													Source of the chemical information /IN Studies References*
		SiO_2	**Al_2O_3**	**Fe_2O_3(t)**	**MnO**	**MgO**	**CaO**	**Na_2O**	**K_2O**	**TiO_2**	**P_2O_5**	**SO_3**	**Cr_2O_3**	**NiO**	
Astroni, Italy (Europe)	AST	59.27	18.80	4.20	0.14	0.88	3.19	3.93	8.51	0.50	0.17	0.04	0.00	0.00	This study
Chaiten, Chile (South America)	CHA	77.10	13.10	1.12	0.00	0.00	1.27	4.38	2.94	0.04	-	-	-	-	Vogel et al., 2017 / This study
Cordon Caulle, Argentina (South America)	COC	70.49	13.87	3.94	0.11	0.44	1.81	5.09	2.89	0.55	0.10	0.01	0.00	0.00	This study
Da'Ure, Ethiopia (Africa)	DAU	72.81	12.36	3.66	0.09	0.29	1.02	4.61	4.35	0.30	0.04	0.02	0.00	0.00	This study
Etna, Italy (Europe)	ET1	48.38	16.71	11.61	0.21	4.99	9.55	4.03	1.80	1.77	0.65	0.02	0.01	0.00	This study
Etna, Italy (Europe)	ET2	48.82	17.73	10.96	0.18	4.74	9.64	3.85	2.06	1.71	0.61	0.03	0.01	0.00	This study
Mt. Kelud, Indonesia (Asia)	KEL	56.10	19.20	4.89	0.00	5.83	9.54	3.01	0.15	2.70	-	-	-	-	Vogel et al., 2017 / This study
Laacher See, Germany (Europe)	LAS	58.29	21.84	2.45	0.35	0.16	0.95	8.90	5.65	0.26	0.04	0.08	0.00	0.00	This study
Mount St. Helens, USA (North America)	MSH	64.95	17.33	4.60	0.07	1.58	4.74	4.72	1.37	0.63	0.14	0.01	0.00	0.00	This study/ Fornea et al., 2009
Pavlof, Alaska, USA (North America)	PAV	53.23	18.73	9.14	0.19	4.28	8.72	3.58	0.69	1.16	0.28	-	-	-	https://pubs.usgs.gov/sir/2017/5129/sir20175129.pdf / This study
Mt. Sakurajima, Japan (Asia)	SA1	58.91	16.88	7.96	0.16	3.48	7.40	3.04	1.36	0.79	0.16	0.08	0.00	0.00	This study
Mt. Sakurajima, Japan (Asia)	SA2	58.91	16.88	7.96	0.16	3.48	7.40	3.04	1.36	0.79	0.16	0.08	0.00	0.00	This study
Tungurahua, Ecuador (South America)	TU1	58.91	16.88	7.96	0.16	3.48	7.40	3.04	1.36	0.79	0.16	0.08	0.00	0.00	This study
Tungurahua, Ecuador (South America)	TU2	59.39	17.49	6.25	0.10	3.17	6.49	4.11	1.88	0.86	0.24	0.02	0.01	0.00	This study
Unzen, Japan (Asia)	UNN	64.78	16.42	4.67	0.10	2.36	5.39	3.64	2.10	0.59	0.16	0.01	0.01	0.01	This study
Eyjafjallajökull, Iceland (Europe)	EJA	61.20	14.70	8.25	0.00	2.13	4.92	5.26	1.66	1.75	-	-	-	-	Vogel et al., 2017 / Steinke et al., 2011, Hoyle et al., 2011
Soufrière Hills, Montserrat (Europe)	SOU	68.40	15.90	2.83	0.03	2.71	4.61	4.10	1.31	0.02	-	-	-	-	Vogel et al., 2017 / Mangan et al., 2017, Schill et al., 2015, Jahn et al., 2019

Fuego, Guatemala (North America)	FGO	50.49	19.43	10.35	0.00	5.01	9.03	3.41	0.76	-	-	-	-	-	Schill et al., 2015/ Jahn et al., 2019
Oruanui, New Zealand, (Oceania)	ORA	74.15	14.24	2.12	0.07	0.32	1.90	4.17	2.72	0.25	0.05	-	-	-	Schill et al., 2015 / Durant et al., 2008
Mt. St. Helens, USA (North America)	MSH	68.60	17.10	2.67	0.00	0.82	3.58	5.30	1.76	0.17	-	-	-	-	Vogel et al., 2017 / Fornea et al., 2009
Banco Bonito, New Mexico (North America)	OB2	73.05	13.74	2.23	0.05	0.70	1.64	3.94	4.21	0.36	0.08	-	-	-	Genareau et al., 2018
Taupo caldera, New Zealand (Oceania)	TAU	73.48	13.81	2.58	0.10	0.37	1.77	4.72	2.78	0.32	0.06	-	-	-	Genareau et al., 2018
Lathrop Wells, USA (North America)	NIW	48.43	16.22	11.92	0.19	7.04	8.07	3.38	1.70	1.89	1.16	-	-	-	Genareau et al., 2018
Lathrop Wells§, USA (North America)	ONW	49.12	17.14	11.36	0.18	5.73	8.46	3.22	1.73	1.90	1.16	-	-	-	Genareau et al., 2018
Lathrop Wells**, USA (North America)	PNW	49.29	17.09	11.51	0.18	5.68	7.96	3.40	1.87	1.98	1.05	-	-	-	Genareau et al., 2018
Lipari, Italy (Europe)	LIP	75.50	13.00	1.60	0.10	0.00	0.80	3.70	5.20	0.10	0.00	-	-	-	Maters et al., 2019
Colima, Mexico, (South America)	COL	61.70	18.90	4.40	0.10	1.90	5.90	4.90	1.40	0.50	0.20	-	-	-	Maters et al., 2019
Tungurahua, Ecuador (South America)	TUN	59.40	17.50	6.30	0.10	3.20	6.50	4.10	1.90	0.90	0.20	-	-	-	Maters et al., 2019
Sete Cidades, Portugal, (Europe)	CID	62.40	17.40	4.20	0.20	0.90	1.50	7.00	5.30	0.90	0.20	-	-	-	Maters et al., 2019
Astroni, Italy (Europe)	AST	59.50	18.90	4.20	0.10	0.90	3.20	4.00	8.60	0.50	0.20	-	-	-	Maters et al., 2019
Monte Nuovo, Italy, (Europe)	NUO	60.30	19.90	3.30	0.20	0.20	1.90	6.40	7.20	0.40	0.00	-	-	-	Maters et al., 2019
Laacher See, Germany (Europe)	LAC	59.00	21.30	2.50	0.30	0.30	1.10	9.40	5.60	0.30	0.10	-	-	-	Maters et al., 2019
Mount Etna, Italy, (Europe)	ETN	47.70	17.30	11.30	0.20	5.20	10.40	3.60	2.00	1.70	0.60	-	-	-	Maters et al., 2019
Kilauea, Hawaii (North America)	KIL	50.40	13.20	12.40	0.20	8.00	10.40	2.20	0.50	2.40	0.20	-	-	-	Maters et al., 2019 / Durant et al., 2008
Santiaguito, Guatemala (North America)	SAN	42.10	11.60	14.10	-	14.80	10.60	2.50	0.40	2.30	-	-	-	-	Jahn et al., 2019 / Rose et al., 1980
Cerro Hudson, Chile, (South America)	HUD	64.30	15.61	1.37	0.12	1.02	1.99	5.96	3.21	0.92	0.24	-	-	-	Durant et al., 2008 / Naranio and Stern, 1998
Atilan, Guatemala (North America)	ATI	43.10	11.70	13.40	-	14.20	10.60	ND	ND	2.80	-	-	-	-	Durant et al., 2008 / Rose et al., 1980
Ogallala, Nebraska, (North America)	OGA	NA***	NA	NA	NA	NA	NA	NA	NA	NA	NA	NA	NA	NA	Durant et al., 2008
Crater Peak, Alaska, (North America)	CRA	56.88	18.33	7.20	0.14	4.61	7.25	3.32	1.20	0.84	0.23	-	-	-	Durant et al., 2008 / Nye and Turner, 1990
Santorini, Greece, (Europe)	SAT	77.33	12.47	0.77 (as FeO)	-	-	0.30	4.42	4.59	-	-	-	-	-	Gibbs et al., 2015 / Fleet et al., 1999

*Other studies that volcanic ash sample from the same volcano has been used for ice nucleation studies.
§PNW is from the same Lathrop Wells but contains accidental lithics.
**ONW is from the same Lathrop Wells but contains oxidized scoria.
***NA = Data not available.

Table S1. Names, sources, and chemical compositions of volcanic ash particles investigated for their ice nucleation properties from 2008 - 2019.

References

Fleet R E Holdsworth A C Morton M S Stoker, A. J.: Geological Society Special Publications Series Editor, Santorini Volcano. Geological Society., 1999.

Naranio, J. A. and Stern, C. R.: Holocene explosive activity of Hudson Volcano, southern Andes,

Bull. Volcanol., 59(4), 291–306, doi:10.1007/s004450050193, 1998.

Nye, C. J. and Turner, D. L.: Petrology, geochemistry, and age of the Spurr volcanic complex, eastern Aleutian arc, Bull. Volcanol., 52(3), 205–226, doi:10.1007/BF00334805, 1990.

Rose, W. I., Penfield, G. T., Drexler, J. W. and Larson, P. B.: Geochemistry of the andesite flank lavas of three composite cones within the Atitlán Cauldron, Guatemala, Bull. Volcanol., 43(1), 131–153, doi:10.1007/BF02597617, 1980.